Acta Cryst E
CRYSTALLOGRAPHIC COMMUNICATIONS
ISSN 2056-9890

Crystal structure of $CaSiF_6 \cdot 2H_2O$(*mP*2) and reevaluation of the Si^{IV}–F bond-valence parameter R_0

Klemen Motaln[a,b] and Matic Lozinšek[a,b]*

[a]Jožef Stefan Institute, Jamova cesta 39, 1000 Ljubljana, Slovenia, and [b]Jožef Stefan International Postgraduate School, Jamova cesta 39, 1000 Ljubljana, Slovenia. *Correspondence e-mail: matic.lozinsek@ijs.si

Received 17 October 2023
Accepted 25 October 2023

Edited by W. T. A. Harrison, University of Aberdeen, United Kingdom

Keywords: calcium hexafluoridosilicate; bond-valence parameter; crystal structure; disorder; hydrogen bonding.

CCDC reference: 2303630

Supporting information: this article has supporting information at journals.iucr.org/e

The structure of a second polymorph of $CaSiF_6 \cdot 2H_2O$ [calcium hexafluoridosilicate dihydrate; space group *P*2/*c* (No. 13), Pearson symbol *mP*2] was elucidated by single-crystal X-ray diffraction. It arose as an unexpected product when soda-lime glass was attacked by HF. Its crystal structure consists of infinite $^2_\infty[Ca(H_2O)_{2/1}(SiF_6)_{4/4}]$ layers oriented parallel to the *bc*-crystallographic plane, a unique motif among structurally characterized hydrated hexafluoridosilicates. The crystal structure also exhibits inter- and intralayer hydrogen bonds, with the interlayer O—H···O hydrogen bonds involving a disordered hydrogen atom. The large deviation between the calculated bond-valence sum for Si and the expected value prompted a redetermination of the empirical Si^{IV}–F bond-valence parameter R_0. Based on a data set of 42 high-quality crystal structures containing 49 independent Si^{IV} coordination environments, a revised value of 1.534 Å was derived for R_0.

1. Chemical context

Calcium hexafluoridosilicate ($CaSiF_6$) and its hydrated form, calcium hexafluoridosilicate dihydrate ($CaSiF_6 \cdot 2H_2O$), are both commercially available chemicals that have found numerous uses, including as additives for cement manufacture (Smart & Roy, 1979), improving dentine remediation treatments (Kawasaki *et al.*, 1996), and as precursors for synthesis of luminescent materials (Kubus & Meyer, 2013). Although the synthesis of $CaSiF_6 \cdot 2H_2O$ and its dehydration to $CaSiF_6$ were investigated more than 90 years ago (Carter, 1932), their crystal structures were determined relatively recently by laboratory-based powder X-ray diffraction using simulated annealing and Rietveld refinement (Frisoni *et al.*, 2011). The study revealed that $CaSiF_6 \cdot 2H_2O$ crystallizes in the monoclinic crystal system (space group $P2_1/n$, Pearson symbol *mP*4) and exhibits a three-dimensional framework structure. In this work, the crystal structure of a second polymorph of $CaSiF_6 \cdot 2H_2O$ (space group *P*2/*c*, Pearson symbol *mP*2) was determined by low-temperature single-crystal X-ray diffraction. The observed discrepancies between the calculated and expected bond-valence sum (BVS) for Si also provided the impetus for a reevaluation of the Si^{IV}–F bond-valence parameter R_0 and an improved value of R_0 was determined.

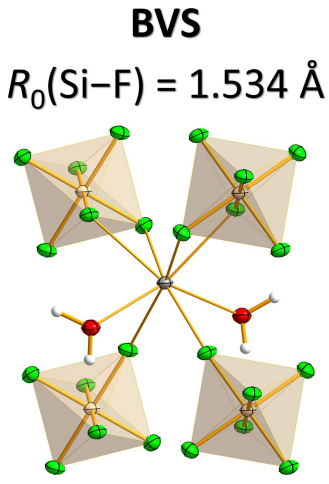

2. Structural commentary

The crystal structure of $CaSiF_6 \cdot 2H_2O$(*mP*2) features eight atoms in the asymmetric unit, with one hydrogen atom disordered over two positions. The Ca atom is located on a twofold rotation axis and the Si atom is situated on an inver-

OPEN ACCESS
Published under a CC BY 4.0 licence

Table 1
Selected bond lengths (Å).

Ca1—F1	2.2965 (9)	Si1—F1	1.6809 (9)
Ca1—F2^{i}	2.3783 (9)	Si1—F2	1.6827 (9)
Ca1—F3^{i}	2.4105 (9)	Si1—F3	1.6942 (9)
Ca1—O1	2.4331 (13)		

Symmetry code: (i) $x, -y+1, z-\frac{1}{2}$.

Table 2
Hydrogen-bond geometry (Å, °).

D—H···A	D—H	H···A	D···A	D—H···A
O1—H1···F3^{ii}	0.78 (3)	2.19 (3)	2.9042 (14)	153 (3)
O1—H2B···O1^{iii}	0.90 (5)	1.98 (5)	2.856 (3)	167 (4)
O1—H2A···O1^{iv}	0.77 (5)	2.17 (5)	2.902 (3)	159 (4)

Symmetry codes: (ii) $-x, -y, -z+1$; (iii) $-x+1, -y+1, -z+1$; (iv) $-x+1, y, -z+\frac{1}{2}$.

sion centre, whereas the light atoms all lie on general positions. The hexafluoridosilicate anion displays a nearly ideal octahedral coordination, with the *cis*-F—Si—F angles ranging from 88.37 (4) to 91.63 (4)°. The average Si—F bond length is 1.6859 Å (Table 1), with the bond lengths ranging from 1.6808 (9) to 1.6942 (9) Å, which is in good agreement with the Si—F distances observed in the crystal structures of $CaSiF_6{\cdot}2H_2O$($mP4$) (Frisoni *et al.*, 2011) and $SrSiF_6{\cdot}2H_2O$ (Golovastikov & Belov, 1982), which span from 1.648 (4) to 1.701 (3) Å and 1.675 (5) to 1.700 (5) Å, respectively. The Ca atom is coordinated by six fluorine atoms at distances of 2.2965 (9)–2.4105 (9) Å originating from four neighbouring $[SiF_6]^{2-}$ octahedra, two of which are bound to the metal centre in a bidentate and two in a monodentate manner. In turn, each $[SiF_6]^{2-}$ octahedron is coordinated to four Ca^{2+} cations. The primary coordination sphere of the Ca^{2+} cation is completed by two water molecules, with a Ca—O distance of 2.4331 (13) Å, resulting in a distorted square antiprismatic coordination (Fig. 1). Such connectivity leads to the formation of $^{2}_{\infty}[Ca(H_2O)_{2/1}(SiF_6)_{4/4}]$ (Jensen, 1989) infinite layers, which extend along the *bc*-crystallographic plane and are stacked along the *a*-axis (Fig. 2), a structural motif that differs from all other hydrated hexafluoridosilicates. Bond-valence sum calculations (Brown, 2009) for Ca and Si using the parameters $b = 0.37$, $R_0 = 1.842$ Å (Ca–F), $R_0 = 1.967$ Å (Ca–O), and $R_0 = 1.58$ Å (Si–F) obtained from the literature (Brown 2020; Brown & Altermatt, 1985; Brese & O'Keeffe, 1991), yielded 2.05 valence units (v.u.) for Ca and 4.51 v.u. for Si (expected values: 2 for Ca, 4 for Si). Similarly inflated values for the bond-valence sum of Si were also observed when other crystal structures of hexafluoridosilicates were examined, indicating the need to reevaluate the current Si^{IV}–F parameter R_0 (Section 5).

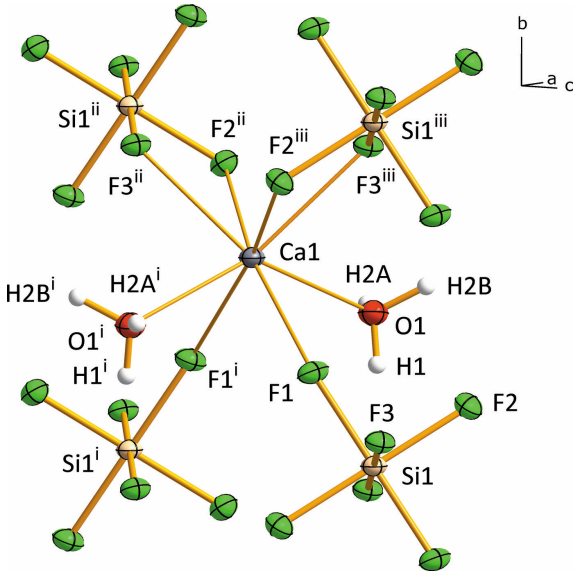

Figure 1
The distorted square antiprismatic coordination environment of the Ca^{2+} cation in the crystal structure of $CaSiF_6{\cdot}2H_2O$($mP2$). Displacement ellipsoids are drawn at the 50% probability level and hydrogen atoms shown as spheres of arbitrary radius. Hydrogen atom H2 is disordered over two sites with occupancies 0.49 (5) and 0.51 (5) [Symmetry codes: (i) $-x, y, -z+\frac{1}{2}$; (ii) $x, -y+1, z-\frac{1}{2}$; (iii) $-x, -y+1, -z+1$.]

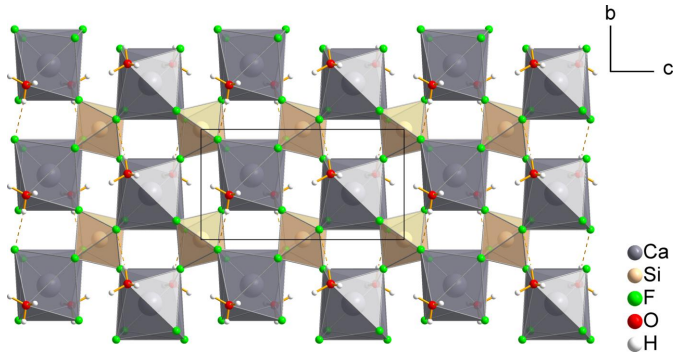

Figure 2
A single $^{2}_{\infty}[Ca(H_2O)_{2/1}(SiF_6)_{4/4}]$ layer viewed along [100], with the intralayer O—H···F hydrogen bonds depicted as dashed lines.

3. Supramolecular features

The crystal structure of $CaSiF_6{\cdot}2H_2O$($mP2$) exhibits both intralayer O—H···F and interlayer O—H···O hydrogen bonds (Table 2, Fig. 3). The intralayer hydrogen bonds are

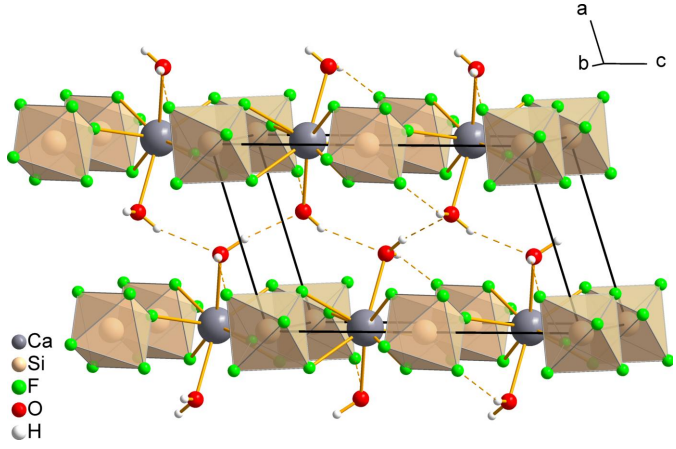

Figure 3
Selected fragment of the crystal structure of $CaSiF_6{\cdot}2H_2O$($mP2$) displaying intra- and interlayer hydrogen bonds, which connect the adjacent layers. Some of the disordered hydrogen atoms have been omitted for clarity.

formed between the F3 atom and the non-disordered hydrogen atom H1, with an O1···F3 distance of 2.9042 (14) Å and a graph-set motif of $S(6)$ (Etter *et al.*, 1990). The oxygen atom O1 is involved in two further hydrogen bonds with the disordered hydrogen atoms H2*A* and H2*B*, forming O1—H2*A*···O1 and O1—H2*B*···O1 hydrogen bonds, with O···O distances of 2.902 (3) and 2.856 (3) Å, respectively, that link the adjacent $^{2}_{\infty}[Ca(H_2O)_{2/1}(SiF_6)_{4/4}]$ layers.

4. Database survey

A search of the Inorganic Crystal Structure Database (ICSD, version January 2023; Bergerhoff *et al.*, 1983; Zagorac *et al.*, 2019) revealed that in addition to the aforementioned *mP*4 polymorph of $CaSiF_6{\cdot}2H_2O$, twelve other hydrated hexafluoridosilicates of divalent cations have been crystallographically characterized to date. Most of them form hexahydrates with the general formula $MSiF_6{\cdot}6H_2O$, where *M* = Mg (Syoyama & Osaki, 1972; Cherkasova *et al.*, 2004), Cr (Cotton *et al.*, 1992), Mn (Torii *et al.*, 1997), Fe (Hamilton, 1962; Chevrier *et al.*, 1981), Co (Lynton & Siew; 1973; Ray *et al.*, 1973*a*; Ray & Mostafa, 1996), Ni (Ray *et al.*, 1973*a*), Cu (Ray *et al.*, 1973*b*), and Zn (Ray *et al.*, 1973*a*). The aforementioned compounds all exhibit a similar structural motif composed of alternating discrete $[M(H_2O)_6]^{2+}$ and $[SiF_6]^{2-}$ octahedra, connected *via* O—H···F hydrogen bonds into a three-dimensional network. The only examples of tetrahydrated metal(II) hexafluoridosilicates are the isostructural $CrSiF_6{\cdot}4H_2O$ (Cotton *et al.*, 1993) and $CuSiF_6{\cdot}4H_2O$ (Clark *et al.*, 1969; Schnering & Vu, 1983; Troyanov *et al.*, 1992; Cotton *et al.*, 1993). In their crystal structures, infinite zigzag chains are formed by the coordination of two $[SiF_6]^{2-}$ octahedra to the apical positions of the square-planar $[M(H_2O)_4]^{2+}$ units. The resulting highly distorted octahedral coordination surrounding the metal centre is characteristic of the Jahn–Teller active cations. The individual chains in the structures are connected by O—H···F hydrogen bonds that link the terminal fluorine atoms of the $[SiF_6]^{2-}$ units to the water molecules coordinating the metal centres of the adjacent chains. Lastly there are three examples of metal(II) hexafluoridosilicate dihydrates, the isostructural pair $CaSiF_6{\cdot}2H_2O$(*mP*4) (Frisoni *et al.*, 2011) and $SrSiF_6{\cdot}2H_2O$ (Golovastikov & Belov, 1982), and $PbSiF_6{\cdot}2H_2O$ (Golubev *et al.*, 1991). All three compounds feature an extended three-dimensional framework structure and display water molecules bridging the metal centres, giving rise to dimeric $[(H_2O)M(\mu\text{-}H_2O)_2\text{-}M(OH_2)]^{4+}$ units for *M* = Ca, Sr and the more complex $[Pb_4(H_2O)_6]^{8+}$ units in the structure of $PbSiF_6{\cdot}2H_2O$, which contain both μ- and μ_3-water molecules. The Ca^{2+} cation in $CaSiF_6{\cdot}2H_2O$(*mP*4) is coordinated by five fluorine and three oxygen atoms arranged in a distorted square-antiprismatic coordination. Each of the five fluorine atoms coordinated to the Ca^{2+} ion belongs to a separate $[SiF_6]^{2-}$ octahedron, which contrasts with the structure of the newly discovered *mP*2 polymorph, where both monodentate and bidentate coordination of the $[SiF_6]^{2-}$ anions to the Ca^{2+} cations is observed (Fig. 4). Conversely, each $[SiF_6]^{2-}$ anion in the structure of $CaSiF_6{\cdot}2H_2O$(*mP*4) coordinates five neighbouring Ca^{2+} cations, leaving one terminal fluorine atom, which in turn accepts O—H···F hydrogen bonds from two water ligands.

5. Redetermination of Si^{IV}–F bond-valence parameter R_0

In order to determine a more accurate value of the Si^{IV}–F bond-valence parameter R_0, the ICSD was searched for all crystal structures containing Si^{IV} in an exclusively fluorine environment. To ensure that only high-quality data were used for the calculation of the R_0 parameter, the data set was limited to crystal structures solved by single-crystal X-ray diffraction at ambient or low-temperature conditions, excluding disordered structures or those with an R_1-value above 0.05. A data set of 42 crystal structures was obtained, containing a total of 49 independent Si^{IV} coordination envir-

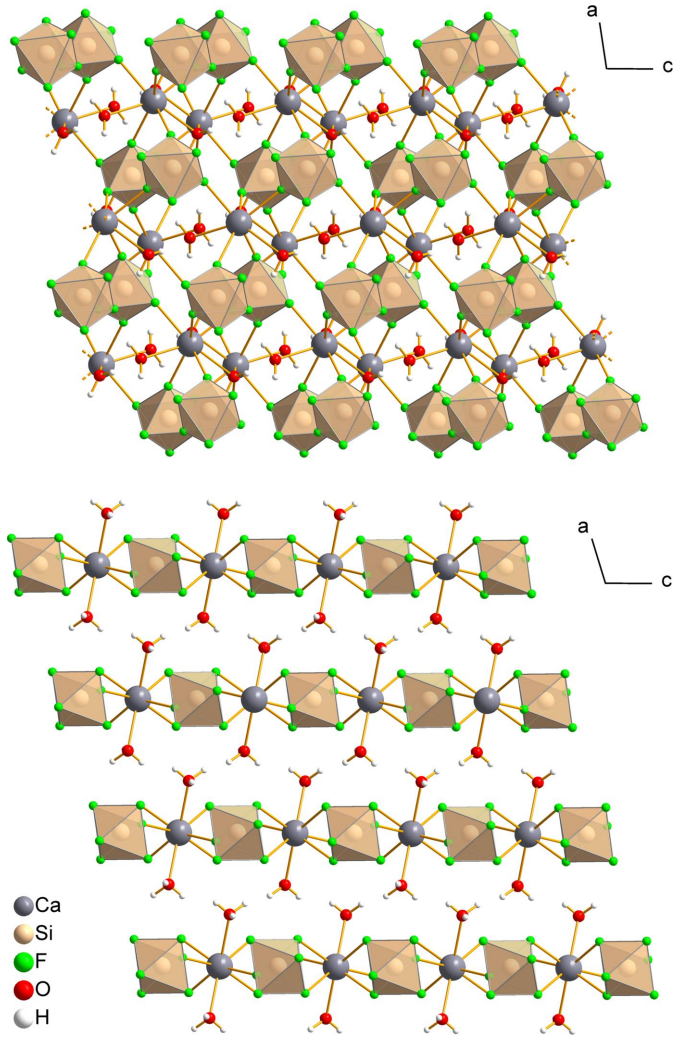

Figure 4
Comparison of the crystal structures of $CaSiF_6{\cdot}2H_2O$(*mP*4) (top) and $CaSiF_6{\cdot}2H_2O$(*mP*2) (bottom), viewed along [010].

Table 3
Crystal structures used for the calculation of the new empirical R_0 bond-valence parameter for Si^{IV}–F.

Compound	ICSD number	Reference	Si—F bond-length range (Å)	BVS for Si (R_0 from Brese & O'Keeffe, 1991)	BVS for Si (new R_0)
$BaSiF_6$	60882	(Svensson *et al.*, 1986)	1.688 (2)	4.481	3.968
$(CH_3NH_3)_2SiF_6$	110673	(Conley *et al.*, 2002)	1.6810 (12)–1.6828 (17)	4.559	4.037
$(CH_7N_4)_2SiF_6{\cdot}2H_2O$	280103	(Ross *et al.*, 1999)	1.6797 (9)–1.6808 (9)	4.578	4.054
$(CH_8N_4)SiF_6$	280102	(Ross *et al.*, 1999)	1.6684 (9)–1.7043 (9)	4.529	4.010
$(C(NH_2)_2OH)_2SiF_6$	63069	(Gubin *et al.*, 1988)	1.677 (2)–1.6971 (18)	4.513	3.996
$(C(NH_2)_3)_2SiF_6$	59237	(Waskowska, 1997)	1.6805 (12)–1.6833 (8)	4.550	4.029
$(C_4H_{13}N_5)SiF_6$	166449	(Gel'mbol'dt *et al.*, 2009)	1.657 (3)–1.698 (3)	4.643	4.111
$CaSiF_6{\cdot}2H_2O$(*mP*2)	Present work		1.6808 (9)–1.6942 (9)	4.507	3.991
$[Co(NH_3)_5(NO_2)]SiF_6$	280030	(Naumov *et al.*, 1999)	1.6769 (18)–1.6899 (13)	4.495	3.981
$CrSiF_6{\cdot}4H_2O$	165384	(Cotton *et al.*, 1993)	1.6640 (8)–1.6968 (8)	4.546	4.026
$CsLiSiF_6$	142874	(Stoll *et al.*, 2021)	1.667 (2)–1.699 (2)	4.479	3.966
$[Cu(bpy)_2(H_2O)]SiF_6{\cdot}4H_2O$	133607	(Nisbet *et al.*, 2021)	1.6677 (10)–1.6947 (9)	4.574	4.050
$[Cu\{SC(NH_2)_2\}_4]_2SiF_6$	249750	(Bowmaker *et al.*, 2008)	1.663 (2)–1.696 (2)	4.585	4.060
$CuSiF_6{\cdot}4H_2O$	165385	(Cotton *et al.*, 1993)	1.6686 (8)–1.6973 (9)	4.510	3.993
$CuSiF_6{\cdot}6H_2O$	34760	(Ray *et al.*, 1973*b*)	1.679 (5)	4.591	4.066
			1.659 (6)–1.674 (6)	4.765	4.219
$H_2SiF_6{\cdot}4H_2O$	40388	(Mootz & Oellers, 1988)	1.666 (1)–1.696 (1)	4.553	4.031
$H_2SiF_6{\cdot}6H_2O$	40389	(Mootz & Oellers, 1988)	1.677 (1)–1.704 (1)	4.447	3.938
$H_2SiF_6{\cdot}9.5H_2O$	40390	(Mootz & Oellers, 1988)	1.680 (1)–1.697 (1)	4.454	3.944
			1.684 (1)–1.706 (1)	4.448	3.939
K_2SiF_6(*cF*4)	420429	(Kutoglu *et al.*, 2009)	1.6873 (16)	4.490	3.975
K_2SiF_6(*hP*2)	158483	(Gramaccioli & Campostrini, 2007)	1.681 (2)–1.689 (2)	4.518	4.000
$K_2SiF_6{\cdot}KNO_3$	417735	(Rissom *et al.*, 2008)	1.6782 (6)	4.601	4.074
$KLiSiF_6$	142875	(Stoll *et al.*, 2021)	1.676 (1)–1.701 (1)	4.495	3.980
$KNaSiF_6$	71334	(Fischer & Krämer, 1991)	1.641 (5)–1.678 (5)	4.860	4.304
$K_3Na(SiF_6)(TaF_7)$	122403	(Tang *et al.*, 2021)	1.665 (3)–1.702 (3)	4.558	4.036
$K_3Na_4(BF_4)(SiF_6)_3$	121301	(Bandemehr *et al.*, 2020)	1.650 (2)–1.699 (2)	4.535	4.015
			1.666 (2)–1.700 (1)	4.560	4.038
Li_2SiF_6	425923	(Hinteregger *et al.*, 2014)	1.685 (2)	4.518	4.000
			1.690 (2)–1.690 (8)	4.457	3.947
$MgSiF_6{\cdot}6H_2O$	250196	(Cherkasova *et al.*, 2004)	1.6888 (9)–1.7465 (10)	4.194	3.714
$MnSiF_6{\cdot}6H_2O$	59274	(Torii *et al.*, 1997)	1.690 (7)	4.457	3.947
			1.668 (7)–1.693 (7)	4.575	4.051
$(NH_3OH)_2SiF_6{\cdot}2H_2O$	94567	(Kristl *et al.*, 2002)	1.6793 (10)–1.6837 (10)	4.570	4.046
$(NH_4)_2SiF_6$	54724	(Fábry *et al.*, 2001)	1.695 (1)–1.700 (1)	4.368	3.867
$(N_2H_5)_2SiF_6$	776	(Ouasri *et al.*, 2019)	1.6777 (4)–1.7101 (4)	4.476	3.963
$(N_2H_6)SiF_6$	35702	(Cameron *et al.*, 1983)	1.671 (1)–1.683 (1)	4.596	4.070
Na_2SiF_6	433134	(Zhang *et al.*, 2017)	1.6755 (14)–1.6756 (14)	4.635	4.104
			1.6907 (16)–1.6916 (11)	4.443	3.934
$PbSiF_6{\cdot}2H_2O$	39358	(Golubev *et al.*, 1991)	1.645 (10)–1.707 (10)	4.558	4.036
			1.664 (10)–1.716 (10)	4.411	3.906
Rb_2SiF_6	136303	(Rienmüller *et al.*, 2021)	1.693 (3)	4.421	3.915
$[RuF(NH_3)_4(NO)]SiF_6$	703	(Mikhailov *et al.*, 2019)	1.661 (1)–1.713 (2)	4.556	4.035
$[Ru_2(H_2O)_2(NH_4)_8S_2](SiF_6)_2$	111446	(Woods & Wilson, 2021)	1.666 (2)–1.7065 (19)	4.552	4.031
SiF_4	48147	(Mootz & Korte, 1984)	1.5401 (6)	4.455	3.945
$SrSiF_6{\cdot}2H_2O$	20552	(Golovastikov & Belov, 1982)	1.675 (5)–1.700 (5)	4.502	3.987
$[Tl_2(NH_3)_6]SiF_6{\cdot}2NH_3$	144214	(Rudel *et al.*, 2021)	1.687 (2)–1.6877 (15)	4.488	3.974
Tl_2SiF_6	136300	(Rienmüller *et al.*, 2021)	1.686 (6)	4.505	3.989
$Tl_3F[SiF_6]$	136302	(Rienmüller *et al.*, 2021)	1.688 (6)–1.695 (6)	4.439	3.931

onments, including the compound presented herein (Table 3). The R_{0i} value for each individual Si coordination environment was calculated using formula (A1.3) from the literature (Brown, 2002), which assumes a fixed value for the *b* parameter (0.37 Å). An improved value for the R_0 parameter, 1.534 Å, was obtained by averaging the R_{0i} values, which ranged from 1.508 to 1.562 Å. BVS calculations employing the new empirical parameter yield significantly improved results compared to the calculations performed with the previously reported parameter, as 46 out of 49 evaluated coordination environments give a bond-valence sum within ±0.2 v.u. of the expected value (3.8–4.2 v.u.), in contrast to only a single one when using the old parameter (Table 4).

Table 4
Comparison of the BVS calculation results for Si^{IV} of crystal structures collected in Table 3 employing the new R_0 parameter and the previously reported parameter.

	R_0	Maximum BVS	Minimum BVS	Mean BVS	Standard deviation	% of data within ± 0.2 v.u.	% of data within ± 0.1 v.u.
This study	1.534	4.304	3.714	4.005	0.086	93.9	87.8
Brese & O'Keeffe (1991)	1.58	4.860	4.194	4.522	0.098	2.0	0

6. Synthesis and crystallization

Colourless single crystals of the title compound were discovered to have grown serendipitously on a soda-lime watch glass containing a sample of [XeF][SbF_6] (Gillespie & Landa, 1973) frozen under a protective layer of perfluorodecalin at 255 K. It is presumed that $CaSiF_6{\cdot}2H_2O$(*mP*2) formed when the soda-lime glass was attacked by the HF forming during hydrolysis of the highly oxidizing Xe^{II} compound.

7. Raman spectroscopy

A Bruker Senterra II confocal Raman microscope was used to record the Raman spectrum on a randomly oriented single crystal of the title compound. The spectrum was measured at room temperature (297 K) in the 50–4250 cm^{-1} range with a resolution of 4 cm^{-1} using the 532 nm laser line operating at 12.5 mW.

In the Raman spectrum of $CaSiF_6{\cdot}2H_2O$(*mP*2) (Fig. 5) the bands observed at 677 and 500 cm^{-1} correspond to the ν_1 and ν_2 modes of the $[SiF_6]^{2-}$ anion, respectively. The bands at 425 and 392 cm^{-1} can be assigned to the ν_5 mode, split due to the distortion of the anion from the ideal O_h symmetry (Ouasri *et al.*, 2002). The Raman bands observed in the 3300–3600 cm^{-1} region belong to the symmetric ν_1 and antisymmetric ν_3 O—H stretching of the coordinated water molecules, whereas the bands at 1649 and 3225 cm^{-1} could likely be assigned to δ(HOH) (ν_2) and 2δ(HOH), respectively (Lacroix *et al.*, 2018).

8. Refinement

Crystal data, data collection and structure refinement details are summarized in Table 5. The positions of the hydrogen atoms, including the disordered one, were located in difference maps and freely refined, including their isotropic thermal parameter U_{iso} (Cooper *et al.*, 2010). The refinement of the disordered hydrogen atoms' occupancies, resulted in values of 0.51 (5) and 0.49 (5) for H2*A* and H2*B*, respectively.

Funding information

Funding for this research was provided by: European Research Council (ERC) under the European Union's Horizon 2020 research and innovation programme (Grant agreement No. 950625); Jožef Stefan Institute Director's Fund; Slovenian Research and Innovation Agency (N1-0189).

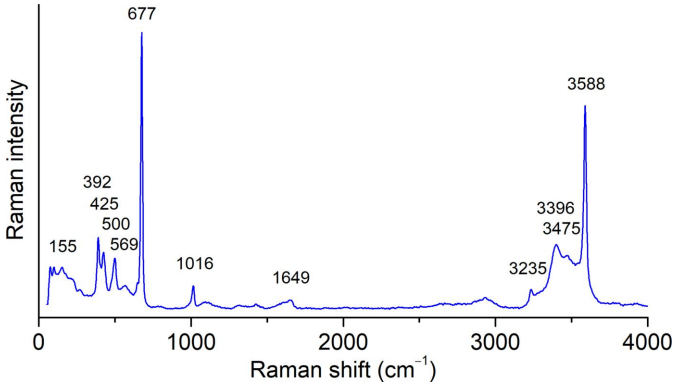

Figure 5
Raman spectrum of $CaSiF_6{\cdot}2H_2O$(*mP*2).

Table 5
Experimental details.

Crystal data	
Chemical formula	$CaSiF_6{\cdot}2H_2O$
M_r	218.20
Crystal system, space group	Monoclinic, *P*2/*c*
Temperature (K)	100
a, *b*, *c* (Å)	5.96605 (17), 5.13977 (12), 9.9308 (3)
β (°)	107.275 (3)
V (Å^3)	290.78 (1)
Z	2
Radiation type	Cu *K*α
μ (mm^{-1})	12.29
Crystal size (mm)	0.15 × 0.08 × 0.02
Data collection	
Diffractometer	XtaLAB Synergy-S, Dualflex, Eiger2 R CdTe 1M
Absorption correction	Gaussian (*CrysAlis PRO*; Rigaku OD, 2022)
T_{min}, T_{max}	0.365, 1.000
No. of measured, independent and observed [$I > 2\sigma(I)$] reflections	8322, 608, 598
R_{int}	0.051
$(\sin \theta/\lambda)_{max}$ (Å^{-1})	0.628
Refinement	
$R[F^2 > 2\sigma(F^2)]$, $wR(F^2)$, *S*	0.025, 0.070, 1.14
No. of reflections	608
No. of parameters	61
H-atom treatment	All H-atom parameters refined
$\Delta\rho_{max}$, $\Delta\rho_{min}$ (e Å^{-3})	0.32, −0.37

Computer programs: *CrysAlis PRO* (Rigaku OD, 2022), *SUPERFLIP* (Palatinus & Chapuis, 2007), *SHELXL2019/2* (Sheldrick, 2015), *OLEX2* (Dolomanov *et al.*, 2009), *DIAMOND* (Brandenburg, 2005) and *publCIF* (Westrip, 2010).

References

Bandemehr, J., Klippstein, J., Ivlev, S., Sachs, M. & Kraus, F. (2020). *Z. Kristallogr.* **235**, 247–254.
Bergerhoff, G., Hundt, R., Sievers, R. & Brown, I. D. (1983). *J. Chem. Inf. Comput. Sci.* **23**, 66–69.
Bowmaker, G. A., Pakawatchai, C., Skelton, B. W., Thanyasirikul, Y. & White, A. H. (2008). *Z. Anorg. Allg. Chem.* **634**, 2583–2588.
Brandenburg, K. (2005). *DIAMOND*. Crystal Impact GbR, Bonn, Germany.
Brese, N. E. & O'Keeffe, M. (1991). *Acta Cryst.* B**47**, 192–197.
Brown, I. D. (2002). *The Chemical Bonding in Inorganic Chemistry: The Bond Valence Model.* Oxford: Oxford University Press.
Brown, I. D. (2009). *Chem. Rev.* **109**, 6858–6919.
Brown, I. D. (2020). bvparam2020.cif, *Accumulated Table of Bond Valence Parameters*, (IUCr) Bond valence parameters, http://www.iucr.org/resources/data/datasets/bond-valence-parameters. Brockhouse Institute for Materials Research, McMaster University, Hamilton, ON, Canada.
Brown, I. D. & Altermatt, D. (1985). *Acta Cryst.* B**41**, 244–247.
Cameron, T. S., Knop, O. & MacDonald, L. A. (1983). *Can. J. Chem.* **61**, 184–188.
Carter, R. H. (1932). *J. Econ. Entomol.* **25**, 707–709.
Cherkasova, T. G., Tatarinova, E. S. & Cherkasova, E. V. (2004). *Zh. Neorg. Khim.* **49**, 1161–1164.
Chevrier, G., Hardy, A. & Jéhanno, G. (1981). *Acta Cryst.* A**37**, 578–584.

Clark, M. J. R., Fleming, J. E. & Lynton, H. (1969). *Can. J. Chem.* **47**, 3859–3861.
Conley, B. D., Yearwood, B. C., Parkin, S. & Atwood, D. A. (2002). *J. Fluorine Chem.* **115**, 155–160.
Cooper, R. I., Thompson, A. L. & Watkin, D. J. (2010). *J. Appl. Cryst.* **43**, 1100–1107.
Cotton, F. A., Daniels, L. M. & Murillo, C. A. (1993). *Inorg. Chem.* **32**, 4868–4870.
Cotton, F. A., Falvello, L. R., Murillo, C. A. & Quesada, J. F. (1992). *J. Solid State Chem.* **96**, 192–198.
Dolomanov, O. V., Bourhis, L. J., Gildea, R. J., Howard, J. A. K. & Puschmann, H. (2009). *J. Appl. Cryst.* **42**, 339–341.
Etter, M. C., MacDonald, J. C. & Bernstein, J. (1990). *Acta Cryst.* B**46**, 256–262.
Fábry, J., Chval, J. & Petříček, V. (2001). *Acta Cryst.* E**57**, i90–i91.
Fischer, J. & Krämer, V. (1991). *Mater. Res. Bull.* **26**, 925–930.
Frisoni, S., Brenna, S. & Masciocchi, N. (2011). *Powder Diffr.* **26**, 308–312.
Gel'mbol'dt, V. O., Minacheva, L. Kh., Ganin, E. V., Sergienko, V. S. & Botoshansky, M. S. (2009). *Zh. Neorg. Khim.* **54**, 1974.
Gillespie, R. J. & Landa, B. (1973). *Inorg. Chem.* **12**, 1383–1389.
Golovastikov, N. I. & Belov, N. V. (1982). *Kristallografiya*, **27**, 1084–1086.
Golubev, A. M., Ilinets, A. M., Tsvigunov, A. N. & Makarevich, L. G. (1991). *Kristallografiya*, **36**, 214–216.
Gramaccioli, C. M. & Campostrini, I. (2007). *Can. Mineral.* **45**, 1275–1280.
Gubin, A. I., Buranbaev, M. Zh., Nurakhmetov, N. N., Suyundikova, F. O. & Tashenov, A. (1988). *Kristallografiya*, **33**, 509–510.
Hamilton, W. C. (1962). *Acta Cryst.* **15**, 353–360.
Hinteregger, E., Wurst, K., Niederwieser, N., Heymann, G. & Huppertz, H. (2014). *Z. Kristallogr.* **229**, 77–82.
Jensen, W. B. (1989). *Cohesion and Structure*, Vol. 2, *The Structures of Binary Compounds*, edited by F. R. de Boer and D. G. Pettifor, pp. 105–146. Amsterdam: North-Holland
Kawasaki, A., Ishikawa, K., Suge, T., Yoshiyama, M., Asaoka, K. & Ebisu, S. (1996). *J. Dent.* **24**, 429–434.
Kristl, M., Drofenik, M. & Golič, L. (2002). *Acta Chim. Slov.* **49**, 243–250.
Kubus, M. & Meyer, H.-J. (2013). *Z. Anorg. Allg. Chem.* **639**, 669–671.
Kutoglu, A., Nikolov, V., Petrov, K. & Allmann, R. (2009). ICSD Communication.
Lacroix, M. R., Bukovsky, E. V., Lozinšek, M., Folsom, T. C., Newell, B. S., Liu, Y., Peryshkov, D. V. & Strauss, S. H. (2018). *Inorg. Chem.* **57**, 14983–15000.
Lynton, H. & Siew, P. Y. (1973). *Can. J. Chem.* **51**, 227–229.
Mikhailov, A., Vuković, V., Kijatkin, C., Wenger, E., Imlau, M., Woike, T., Kostin, G. & Schaniel, D. (2019). *Acta Cryst.* B**75**, 1152–1163.
Mootz, D. & Korte, L. (1984). *Z. Naturforsch. B*, **39**, 1295–1299.
Mootz, D. & Oellers, E. J. (1988). *Z. Anorg. Allg. Chem.* **559**, 27–39.
Naumov, D. Yu., Kashcheeva, N. E., Boldyreva, E. V. & Howard, J. A. K. (1999). *Acta Cryst.* C**55**, 1205–1208.
Nisbet, M. L., Hiralal, E. & Poeppelmeier, K. R. (2021). *Acta Cryst.* E**77**, 158–164.
Ouasri, A., Lambarki, F., Rhandour, A., Saadi, M. & El Ammari, L. (2019). *Acta Cryst.* E**75**, 1507–1510.
Ouasri, A., Rhandour, A., Dhamelincourt, M.-C., Dhamelincourt, P., Mazzah, A. & Taibi, M. (2002). *J. Raman Spectrosc.* **33**, 715–719.
Palatinus, L. & Chapuis, G. (2007). *J. Appl. Cryst.* **40**, 786–790.
Ray, S. & Mostafa, G. (1996). *Z. Kristallogr.* **211**, 368–372.
Ray, S., Zalkin, A. & Templeton, D. H. (1973*a*). *Acta Cryst.* B**29**, 2741–2747.
Ray, S., Zalkin, A. & Templeton, D. H. (1973*b*). *Acta Cryst.* B**29**, 2748–2751.
Rienmüller, J., Bandemehr, J. & Kraus, F. (2021). *Z. Naturforsch. B*, **76**, 559–565.
Rigaku OD (2022). *CrysAlis PRO*. Rigaku Corporation, Wrocław, Poland.
Rissom, C., Schmidt, H. & Voigt, W. (2008). *Cryst. Res. Technol.* **43**, 74–82.
Ross, C. R., Bauer, M. R., Nielson, R. M. & Abrahams, S. C. (1999). *Acta Cryst.* B**55**, 246–254.
Rudel, S. S., Graubner, T., Karttunen, A. J., Dehnen, S. & Kraus, F. (2021). *Inorg. Chem.* **60**, 15031–15040.
Schnering, H. G. von V. & Vu, D. (1983). *Angew. Chem.* **95**, 421.
Sheldrick, G. M. (2015). *Acta Cryst.* C**71**, 3–8.
Smart, R. M. & Roy, D. M. (1979). *Cem. Concr. Res.* **9**, 269–273.
Stoll, C., Seibald, M., Baumann, D., Bandemehr, J., Kraus, F. & Huppertz, H. (2021). *Eur. J. Inorg. Chem.* pp. 62–70.
Svensson, G., Albertsson, J., Svensson, C. & Elding, L. I. (1986). *Acta Chem. Scand.* **40a**, 631–633.
Syoyama, S. & Osaki, K. (1972). *Acta Cryst.* B**28**, 2626–2627.
Tang, R. L., Lian, X., Yao, W. D., Liu, W. & Guo, S. P. (2021). *Dalton Trans.* **50**, 16562–16567.
Torii, A., Ogawa, K., Tamura, H. & Osaki, K. (1997). *Acta Cryst.* C**53**, 833–836.
Troyanov, S. I., Morozov, I. V. & Korenev, Yu. M. (1992). *Zh. Neorg. Khim.* **37**, 380–387.
Waskowska, A. (1997). *Acta Cryst.* C**53**, 128–130.
Westrip, S. P. (2010). *J. Appl. Cryst.* **43**, 920–925.
Woods, J. J. & Wilson, J. J. (2021). *Angew. Chem. Int. Ed.* **60**, 1588–1592.
Zagorac, D., Müller, H., Ruehl, S., Zagorac, J. & Rehme, S. (2019). *J. Appl. Cryst.* **52**, 918–925.
Zhang, W., Jing, Q., Fang, Y. & Chen, Z. (2017). *Z. Anorg. Allg. Chem.* **643**, 1739–1743.

supporting information

Acta Cryst. (2023). E**79**, 1121-1126 [https://doi.org/10.1107/S2056989023009349]

Crystal structure of $CaSiF_6{\cdot}2H_2O$(*mP*2) and reevaluation of the Si^{IV}–F bond-valence parameter R_0

Klemen Motaln and Matic Lozinšek

Computing details

Calcium hexafluoridosilicate dihydrate

Crystal data

$CaSiF{\cdot}2H_2O$
M_r = 218.20
Monoclinic, *P*2/*c*
a = 5.96605 (17) Å
b = 5.13977 (12) Å
c = 9.9308 (3) Å
β = 107.275 (3)°
V = 290.78 (1) Å^3
Z = 2
F(000) = 216
D_x = 2.492 Mg m^{-3}
Cu *Kα* radiation, λ = 1.54184 Å
Cell parameters from 5902 reflections
θ = 7.8–75.3°
μ = 12.29 mm^{-1}
T = 100 K
Plate, colourless
0.15 × 0.08 × 0.02 mm

Data collection

XtaLAB Synergy-S, Dualflex, Eiger2 R CdTe 1M diffractometer
Radiation source: micro-focus sealed X-ray tube, PhotonJet (Cu) X-ray Source
Mirror monochromator
Detector resolution: 13.3333 pixels mm^{-1}
ω scans
Absorption correction: gaussian (CrysalisPro; Rigaku OD, 2022)
T_{min} = 0.365, T_{max} = 1.000
8322 measured reflections
608 independent reflections
598 reflections with $I > 2\sigma(I)$
R_{int} = 0.051
θ_{max} = 75.4°, θ_{min} = 7.8°
$h = -7 \rightarrow 7$
$k = -6 \rightarrow 6$
$l = -12 \rightarrow 12$

Refinement

Refinement on F^2
Least-squares matrix: full
$R[F^2 > 2\sigma(F^2)]$ = 0.025
$wR(F^2)$ = 0.070
S = 1.14
608 reflections
61 parameters
0 restraints
Primary atom site location: iterative
Hydrogen site location: difference Fourier map
All H-atom parameters refined
$w = 1/[\sigma^2(F_o^2) + (0.0516P)^2 + 0.0488P]$ where $P = (F_o^2 + 2F_c^2)/3$
$(\Delta/\sigma)_{max} < 0.001$
$\Delta\rho_{max}$ = 0.32 e Å^{-3}
$\Delta\rho_{min}$ = −0.37 e Å^{-3}

Special details

Geometry. All esds (except the esd in the dihedral angle between two l.s. planes) are estimated using the full covariance matrix. The cell esds are taken into account individually in the estimation of esds in distances, angles and torsion angles; correlations between esds in cell parameters are only used when they are defined by crystal symmetry. An approximate (isotropic) treatment of cell esds is used for estimating esds involving l.s. planes.

Fractional atomic coordinates and isotropic or equivalent isotropic displacement parameters (Å²)

	x	*y*	*z*	U_{iso}*/U_{eq}	Occ. (<1)
Ca1	0.000000	0.58252 (7)	0.250000	0.01360 (19)	
Si1	0.000000	0.000000	0.500000	0.0135 (2)	
F1	−0.06447 (16)	0.26688 (17)	0.39793 (9)	0.0187 (3)	
F2	0.20424 (15)	0.17052 (18)	0.62125 (9)	0.0178 (2)	
F3	−0.19861 (16)	0.09149 (15)	0.58239 (10)	0.0164 (3)	
O1	0.3884 (2)	0.4033 (2)	0.36145 (15)	0.0190 (3)	
H1	0.378 (5)	0.255 (6)	0.373 (3)	0.035 (7)*	
H2B	0.469 (8)	0.483 (9)	0.441 (5)	0.016 (13)*	0.49 (5)
H2A	0.475 (8)	0.419 (7)	0.318 (5)	0.017 (13)*	0.51 (5)

Atomic displacement parameters (Å²)

	U^{11}	U^{22}	U^{33}	U^{12}	U^{13}	U^{23}
Ca1	0.0176 (3)	0.0092 (3)	0.0144 (3)	0.000	0.00529 (18)	0.000
Si1	0.0181 (3)	0.0090 (3)	0.0140 (3)	0.0000 (2)	0.0059 (2)	0.0000 (2)
F1	0.0251 (5)	0.0124 (4)	0.0201 (5)	0.0025 (4)	0.0091 (4)	0.0041 (3)
F2	0.0189 (5)	0.0155 (4)	0.0190 (5)	−0.0010 (3)	0.0056 (4)	−0.0037 (3)
F3	0.0201 (5)	0.0120 (5)	0.0185 (5)	−0.0003 (3)	0.0080 (4)	−0.0020 (3)
O1	0.0199 (6)	0.0145 (6)	0.0224 (6)	−0.0008 (4)	0.0058 (5)	0.0006 (4)

Geometric parameters (Å, º)

Ca1—Si1^{i}	3.2815 (3)	Si1—F1^{vi}	1.6808 (9)
Ca1—Si1^{ii}	3.2815 (3)	Si1—F1	1.6809 (9)
Ca1—F1	2.2965 (9)	Si1—F2^{vi}	1.6826 (9)
Ca1—F1^{iii}	2.2965 (9)	Si1—F2	1.6827 (9)
Ca1—F2^{iv}	2.3783 (9)	Si1—F3	1.6942 (9)
Ca1—F2^{v}	2.3783 (9)	Si1—F3^{vi}	1.6942 (9)
Ca1—F3^{iv}	2.4105 (9)	O1—H1	0.78 (3)
Ca1—F3^{v}	2.4105 (9)	O1—H2B	0.90 (5)
Ca1—O1	2.4331 (13)	O1—H2A	0.77 (5)
Ca1—O1^{iii}	2.4331 (13)		
Si1^{ii}—Ca1—Si1^{i}	98.328 (10)	O1—Ca1—Si1^{i}	112.20 (3)
F1^{iii}—Ca1—Si1^{i}	86.58 (2)	O1^{iii}—Ca1—Si1^{ii}	112.20 (3)
F1—Ca1—Si1^{i}	169.60 (2)	O1^{iii}—Ca1—Si1^{i}	96.74 (3)
F1^{iii}—Ca1—Si1^{ii}	169.60 (2)	O1^{iii}—Ca1—O1	135.49 (6)
F1—Ca1—Si1^{ii}	86.58 (2)	Ca1^{vii}—Si1—Ca1^{v}	180.0
F1—Ca1—F1^{iii}	90.11 (4)	F1—Si1—Ca1^{v}	82.60 (3)

F1—Ca1—F2^{iv}	158.57 (3)	F1—Si1—Ca1^{vii}	97.40 (3)
F1—Ca1—F2^{v}	79.82 (3)	F1^{vi}—Si1—Ca1^{v}	97.40 (3)
F1^{iii}—Ca1—F2^{iv}	79.82 (3)	F1^{vi}—Si1—Ca1^{vii}	82.60 (3)
F1^{iii}—Ca1—F2^{v}	158.57 (3)	F1^{vi}—Si1—F1	180.0
F1—Ca1—F3^{iv}	142.32 (3)	F1^{vi}—Si1—F2^{vi}	89.65 (5)
F1—Ca1—F3^{v}	100.99 (3)	F1—Si1—F2^{vi}	90.35 (5)
F1^{iii}—Ca1—F3^{v}	142.32 (3)	F1—Si1—F2	89.65 (5)
F1^{iii}—Ca1—F3^{iv}	100.99 (3)	F1^{vi}—Si1—F2	90.35 (5)
F1—Ca1—O1	76.07 (4)	F1—Si1—F3	89.83 (4)
F1^{iii}—Ca1—O1^{iii}	76.07 (4)	F1—Si1—F3^{vi}	90.17 (4)
F1^{iii}—Ca1—O1	72.88 (4)	F1^{vi}—Si1—F3	90.17 (4)
F1—Ca1—O1^{iii}	72.88 (4)	F1^{vi}—Si1—F3^{vi}	89.83 (4)
F2^{v}—Ca1—Si1^{ii}	29.44 (2)	F2—Si1—Ca1^{v}	44.00 (3)
F2^{v}—Ca1—Si1^{i}	99.95 (3)	F2—Si1—Ca1^{vii}	136.00 (3)
F2^{iv}—Ca1—Si1^{i}	29.44 (2)	F2^{vi}—Si1—Ca1^{v}	136.00 (3)
F2^{iv}—Ca1—Si1^{ii}	99.95 (3)	F2^{vi}—Si1—Ca1^{vii}	44.00 (3)
F2^{iv}—Ca1—F2^{v}	115.49 (5)	F2^{vi}—Si1—F2	180.0
F2^{iv}—Ca1—F3^{v}	77.00 (3)	F2—Si1—F3^{vi}	91.63 (4)
F2^{v}—Ca1—F3^{v}	58.87 (3)	F2^{vi}—Si1—F3	91.63 (4)
F2^{v}—Ca1—F3^{iv}	77.00 (3)	F2—Si1—F3	88.37 (4)
F2^{iv}—Ca1—F3^{iv}	58.87 (3)	F2^{vi}—Si1—F3^{vi}	88.37 (4)
F2^{v}—Ca1—O1^{iii}	82.87 (4)	F3—Si1—Ca1^{v}	45.25 (3)
F2^{iv}—Ca1—O1^{iii}	121.89 (4)	F3^{vi}—Si1—Ca1^{v}	134.75 (3)
F2^{iv}—Ca1—O1	82.87 (4)	F3—Si1—Ca1^{vii}	134.75 (3)
F2^{v}—Ca1—O1	121.89 (4)	F3^{vi}—Si1—Ca1^{vii}	45.25 (3)
F3^{v}—Ca1—Si1^{ii}	29.94 (2)	F3—Si1—F3^{vi}	180.0
F3^{v}—Ca1—Si1^{i}	87.56 (2)	Si1—F1—Ca1	155.57 (5)
F3^{iv}—Ca1—Si1^{i}	29.94 (2)	Si1—F2—Ca1^{v}	106.56 (4)
F3^{iv}—Ca1—Si1^{ii}	87.56 (2)	Si1—F3—Ca1^{v}	104.81 (4)
F3^{v}—Ca1—F3^{iv}	91.93 (4)	Ca1—O1—H1	110 (2)
F3^{v}—Ca1—O1	75.09 (4)	Ca1—O1—H2B	115 (3)
F3^{v}—Ca1—O1^{iii}	141.61 (4)	Ca1—O1—H2A	114 (3)
F3^{iv}—Ca1—O1	141.61 (4)	H1—O1—H2B	111 (3)
F3^{iv}—Ca1—O1^{iii}	75.09 (4)	H1—O1—H2A	107 (3)
O1—Ca1—Si1^{ii}	96.74 (3)		

Ca1^{v}—Si1—F1—Ca1	115.56 (12)	F2^{vi}—Si1—F1—Ca1	−108.01 (13)
Ca1^{vii}—Si1—F1—Ca1	−64.44 (12)	F2—Si1—F1—Ca1	71.99 (13)
Ca1^{vii}—Si1—F2—Ca1^{v}	180.000 (1)	F2^{vi}—Si1—F3—Ca1^{v}	−170.07 (5)
Ca1^{vii}—Si1—F3—Ca1^{v}	180.000 (1)	F2—Si1—F3—Ca1^{v}	9.93 (5)
F1^{vi}—Si1—F2—Ca1^{v}	−100.32 (4)	F3^{vi}—Si1—F1—Ca1	−19.64 (13)
F1—Si1—F2—Ca1^{v}	79.69 (4)	F3—Si1—F1—Ca1	160.36 (13)
F1—Si1—F3—Ca1^{v}	−79.72 (4)	F3^{vi}—Si1—F2—Ca1^{v}	169.84 (5)
F1^{vi}—Si1—F3—Ca1^{v}	100.28 (4)	F3—Si1—F2—Ca1^{v}	−10.16 (5)

Symmetry codes: (i) −*x*, *y*+1, −*z*+1/2; (ii) *x*, *y*+1, *z*; (iii) −*x*, *y*, −*z*+1/2; (iv) *x*, −*y*+1, *z*−1/2; (v) −*x*, −*y*+1, −*z*+1; (vi) −*x*, −*y*, −*z*+1; (vii) *x*, *y*−1, *z*.

Hydrogen-bond geometry (Å, º)

D—H···*A*	*D*—H	H···*A*	*D*···*A*	*D*—H···*A*
O1—H1···F3^{vi}	0.78 (3)	2.19 (3)	2.9042 (14)	153 (3)
O1—H2*B*···O1^{viii}	0.90 (5)	1.98 (5)	2.856 (3)	167 (4)
O1—H2*A*···O1^{ix}	0.77 (5)	2.17 (5)	2.902 (3)	159 (4)

Symmetry codes: (vi) −*x*, −*y*, −*z*+1; (viii) −*x*+1, −*y*+1, −*z*+1; (ix) −*x*+1, *y*, −*z*+1/2.

supporting information

Acta Cryst. (2023). E**79**, 1121-1126 [https://doi.org/10.1107/S2056989023009349]

Crystal structure of $CaSiF_6{\cdot}2H_2O$(*mP*2) and reevaluation of the Si^{IV}–F bond-valence parameter R_0

Klemen Motaln and Matic Lozinšek

Computing details

Calcium hexafluoridosilicate dihydrate

Crystal data

$CaSiF_6{\cdot}2H_2O$
M_r = 218.20
Monoclinic, *P*2/*c*
a = 5.96605 (17) Å
b = 5.13977 (12) Å
c = 9.9308 (3) Å
β = 107.275 (3)°
V = 290.78 (1) Å^3
Z = 2
F(000) = 216
D_x = 2.492 Mg m^{-3}
Cu *Kα* radiation, λ = 1.54184 Å
Cell parameters from 5902 reflections
θ = 7.8–75.3°
μ = 12.29 mm^{-1}
T = 100 K
Plate, colourless
0.15 × 0.08 × 0.02 mm

Data collection

XtaLAB Synergy-S, Dualflex, Eiger2 R CdTe 1M diffractometer
Radiation source: micro-focus sealed X-ray tube, PhotonJet (Cu) X-ray Source
Mirror monochromator
Detector resolution: 13.3333 pixels mm^{-1}
ω scans
Absorption correction: gaussian (CrysalisPro; Rigaku OD, 2022)
T_{min} = 0.365, T_{max} = 1.000
8322 measured reflections
608 independent reflections
598 reflections with $I > 2\sigma(I)$
R_{int} = 0.051
θ_{max} = 75.4°, θ_{min} = 7.8°
$h = -7 \rightarrow 7$
$k = -6 \rightarrow 6$
$l = -12 \rightarrow 12$

Refinement

Refinement on F^2
Least-squares matrix: full
$R[F^2 > 2\sigma(F^2)]$ = 0.025
$wR(F^2)$ = 0.070
S = 1.14
608 reflections
61 parameters
0 restraints
Primary atom site location: iterative
Hydrogen site location: difference Fourier map
All H-atom parameters refined
$w = 1/[\sigma^2(F_o^2) + (0.0516P)^2 + 0.0488P]$ where $P = (F_o^2 + 2F_c^2)/3$
$(\Delta/\sigma)_{max} < 0.001$
$\Delta\rho_{max}$ = 0.32 e Å^{-3}
$\Delta\rho_{min}$ = −0.37 e Å^{-3}

Special details

Geometry. All esds (except the esd in the dihedral angle between two l.s. planes) are estimated using the full covariance matrix. The cell esds are taken into account individually in the estimation of esds in distances, angles and torsion angles; correlations between esds in cell parameters are only used when they are defined by crystal symmetry. An approximate (isotropic) treatment of cell esds is used for estimating esds involving l.s. planes.

Fractional atomic coordinates and isotropic or equivalent isotropic displacement parameters (Å²)

	x	*y*	*z*	U_{iso}*/U_{eq}	Occ. (<1)
Ca1	0.000000	0.58252 (7)	0.250000	0.01360 (19)	
Si1	0.000000	0.000000	0.500000	0.0135 (2)	
F1	−0.06447 (16)	0.26688 (17)	0.39793 (9)	0.0187 (3)	
F2	0.20424 (15)	0.17052 (18)	0.62125 (9)	0.0178 (2)	
F3	−0.19861 (16)	0.09149 (15)	0.58239 (10)	0.0164 (3)	
O1	0.3884 (2)	0.4033 (2)	0.36145 (15)	0.0190 (3)	
H1	0.378 (5)	0.255 (6)	0.373 (3)	0.035 (7)*	
H2B	0.469 (8)	0.483 (9)	0.441 (5)	0.016 (13)*	0.49 (5)
H2A	0.475 (8)	0.419 (7)	0.318 (5)	0.017 (13)*	0.51 (5)

Atomic displacement parameters (Å²)

	U^{11}	U^{22}	U^{33}	U^{12}	U^{13}	U^{23}
Ca1	0.0176 (3)	0.0092 (3)	0.0144 (3)	0.000	0.00529 (18)	0.000
Si1	0.0181 (3)	0.0090 (3)	0.0140 (3)	0.0000 (2)	0.0059 (2)	0.0000 (2)
F1	0.0251 (5)	0.0124 (4)	0.0201 (5)	0.0025 (4)	0.0091 (4)	0.0041 (3)
F2	0.0189 (5)	0.0155 (4)	0.0190 (5)	−0.0010 (3)	0.0056 (4)	−0.0037 (3)
F3	0.0201 (5)	0.0120 (5)	0.0185 (5)	−0.0003 (3)	0.0080 (4)	−0.0020 (3)
O1	0.0199 (6)	0.0145 (6)	0.0224 (6)	−0.0008 (4)	0.0058 (5)	0.0006 (4)

Geometric parameters (Å, º)

Ca1—Si1^{i}	3.2815 (3)	Si1—F1^{vi}	1.6808 (9)
Ca1—Si1^{ii}	3.2815 (3)	Si1—F1	1.6809 (9)
Ca1—F1	2.2965 (9)	Si1—F2^{vi}	1.6826 (9)
Ca1—F1^{iii}	2.2965 (9)	Si1—F2	1.6827 (9)
Ca1—F2^{iv}	2.3783 (9)	Si1—F3	1.6942 (9)
Ca1—F2^{v}	2.3783 (9)	Si1—F3^{vi}	1.6942 (9)
Ca1—F3^{iv}	2.4105 (9)	O1—H1	0.78 (3)
Ca1—F3^{v}	2.4105 (9)	O1—H2B	0.90 (5)
Ca1—O1	2.4331 (13)	O1—H2A	0.77 (5)
Ca1—O1^{iii}	2.4331 (13)		
Si1^{ii}—Ca1—Si1^{i}	98.328 (10)	O1—Ca1—Si1^{i}	112.20 (3)
F1^{iii}—Ca1—Si1^{i}	86.58 (2)	O1^{iii}—Ca1—Si1^{ii}	112.20 (3)
F1—Ca1—Si1^{i}	169.60 (2)	O1^{iii}—Ca1—Si1^{i}	96.74 (3)
F1^{iii}—Ca1—Si1^{ii}	169.60 (2)	O1^{iii}—Ca1—O1	135.49 (6)
F1—Ca1—Si1^{ii}	86.58 (2)	Ca1^{vii}—Si1—Ca1^{v}	180.0
F1—Ca1—F1^{iii}	90.11 (4)	F1—Si1—Ca1^{v}	82.60 (3)

F1—Ca1—F2^{iv}	158.57 (3)	F1—Si1—Ca1^{vii}	97.40 (3)
F1—Ca1—F2^{v}	79.82 (3)	F1^{vi}—Si1—Ca1^{v}	97.40 (3)
F1^{iii}—Ca1—F2^{iv}	79.82 (3)	F1^{vi}—Si1—Ca1^{vii}	82.60 (3)
F1^{iii}—Ca1—F2^{v}	158.57 (3)	F1^{vi}—Si1—F1	180.0
F1—Ca1—F3^{iv}	142.32 (3)	F1^{vi}—Si1—F2^{vi}	89.65 (5)
F1—Ca1—F3^{v}	100.99 (3)	F1—Si1—F2^{vi}	90.35 (5)
F1^{iii}—Ca1—F3^{v}	142.32 (3)	F1—Si1—F2	89.65 (5)
F1^{iii}—Ca1—F3^{iv}	100.99 (3)	F1^{vi}—Si1—F2	90.35 (5)
F1—Ca1—O1	76.07 (4)	F1—Si1—F3	89.83 (4)
F1^{iii}—Ca1—O1^{iii}	76.07 (4)	F1—Si1—F3^{vi}	90.17 (4)
F1^{iii}—Ca1—O1	72.88 (4)	F1^{vi}—Si1—F3	90.17 (4)
F1—Ca1—O1^{iii}	72.88 (4)	F1^{vi}—Si1—F3^{vi}	89.83 (4)
F2^{v}—Ca1—Si1^{ii}	29.44 (2)	F2—Si1—Ca1^{v}	44.00 (3)
F2^{v}—Ca1—Si1^{i}	99.95 (3)	F2—Si1—Ca1^{vii}	136.00 (3)
F2^{iv}—Ca1—Si1^{i}	29.44 (2)	F2^{vi}—Si1—Ca1^{v}	136.00 (3)
F2^{iv}—Ca1—Si1^{ii}	99.95 (3)	F2^{vi}—Si1—Ca1^{vii}	44.00 (3)
F2^{iv}—Ca1—F2^{v}	115.49 (5)	F2^{vi}—Si1—F2	180.0
F2^{iv}—Ca1—F3^{v}	77.00 (3)	F2—Si1—F3^{vi}	91.63 (4)
F2^{v}—Ca1—F3^{v}	58.87 (3)	F2^{vi}—Si1—F3	91.63 (4)
F2^{v}—Ca1—F3^{iv}	77.00 (3)	F2—Si1—F3	88.37 (4)
F2^{iv}—Ca1—F3^{iv}	58.87 (3)	F2^{vi}—Si1—F3^{vi}	88.37 (4)
F2^{v}—Ca1—O1^{iii}	82.87 (4)	F3—Si1—Ca1^{v}	45.25 (3)
F2^{iv}—Ca1—O1^{iii}	121.89 (4)	F3^{vi}—Si1—Ca1^{v}	134.75 (3)
F2^{iv}—Ca1—O1	82.87 (4)	F3—Si1—Ca1^{vii}	134.75 (3)
F2^{v}—Ca1—O1	121.89 (4)	F3^{vi}—Si1—Ca1^{vii}	45.25 (3)
F3^{v}—Ca1—Si1^{ii}	29.94 (2)	F3—Si1—F3^{vi}	180.0
F3^{v}—Ca1—Si1^{i}	87.56 (2)	Si1—F1—Ca1	155.57 (5)
F3^{iv}—Ca1—Si1^{i}	29.94 (2)	Si1—F2—Ca1^{v}	106.56 (4)
F3^{iv}—Ca1—Si1^{ii}	87.56 (2)	Si1—F3—Ca1^{v}	104.81 (4)
F3^{v}—Ca1—F3^{iv}	91.93 (4)	Ca1—O1—H1	110 (2)
F3^{v}—Ca1—O1	75.09 (4)	Ca1—O1—H2B	115 (3)
F3^{v}—Ca1—O1^{iii}	141.61 (4)	Ca1—O1—H2A	114 (3)
F3^{iv}—Ca1—O1	141.61 (4)	H1—O1—H2B	111 (3)
F3^{iv}—Ca1—O1^{iii}	75.09 (4)	H1—O1—H2A	107 (3)
O1—Ca1—Si1^{ii}	96.74 (3)		

Ca1^{v}—Si1—F1—Ca1	115.56 (12)	F2^{vi}—Si1—F1—Ca1	−108.01 (13)
Ca1^{vii}—Si1—F1—Ca1	−64.44 (12)	F2—Si1—F1—Ca1	71.99 (13)
Ca1^{vii}—Si1—F2—Ca1^{v}	180.000 (1)	F2^{vi}—Si1—F3—Ca1^{v}	−170.07 (5)
Ca1^{vii}—Si1—F3—Ca1^{v}	180.000 (1)	F2—Si1—F3—Ca1^{v}	9.93 (5)
F1^{vi}—Si1—F2—Ca1^{v}	−100.32 (4)	F3^{vi}—Si1—F1—Ca1	−19.64 (13)
F1—Si1—F2—Ca1^{v}	79.69 (4)	F3—Si1—F1—Ca1	160.36 (13)
F1—Si1—F3—Ca1^{v}	−79.72 (4)	F3^{vi}—Si1—F2—Ca1^{v}	169.84 (5)
F1^{vi}—Si1—F3—Ca1^{v}	100.28 (4)	F3—Si1—F2—Ca1^{v}	−10.16 (5)

Symmetry codes: (i) −*x*, *y*+1, −*z*+1/2; (ii) *x*, *y*+1, *z*; (iii) −*x*, *y*, −*z*+1/2; (iv) *x*, −*y*+1, *z*−1/2; (v) −*x*, −*y*+1, −*z*+1; (vi) −*x*, −*y*, −*z*+1; (vii) *x*, *y*−1, *z*.

Hydrogen-bond geometry (Å, º)

D—H···*A*	*D*—H	H···*A*	*D*···*A*	*D*—H···*A*
O1—H1···F3^{vi}	0.78 (3)	2.19 (3)	2.9042 (14)	153 (3)
O1—H2*B*···O1^{viii}	0.90 (5)	1.98 (5)	2.856 (3)	167 (4)
O1—H2*A*···O1^{ix}	0.77 (5)	2.17 (5)	2.902 (3)	159 (4)

Symmetry codes: (vi) −*x*, −*y*, −*z*+1; (viii) −*x*+1, −*y*+1, −*z*+1; (ix) −*x*+1, *y*, −*z*+1/2.